Food Chemistry: X 21 (2024) 101063

Contents lists available at ScienceDirect

Food Chemistry: X

journal homepage: www.sciencedirect.com/journal/food-chemistry-x

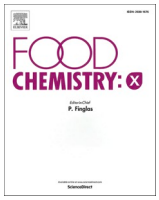

Study of four polyphenol-*Coregonus peled (C. peled)* myofibrillar protein interactions on protein structure and gel properties

Xin Guo [a,b,c], Yabo Wei [a,b,c], Pingping Liu [a,b,c], Xiaorong Deng [a,b,c], Xinrong Zhu [a,b,c], Zhouping Wang [a,*], Jian Zhang [a,b,c,*]

[a] School of Food Science and Technology, Shihezi University, Shihezi, Xinjiang 832003, China
[b] Key Laboratory of Agricultural Product Processing and Quality Control of Specialty (Co-construction by Ministry and Province), School of Food Science and Technology, Shihezi University, Shihezi, Xinjiang 832003, China
[c] Key Laboratory for Food Nutrition and Safety Control of Xinjiang Production and Construction Corps, School of Food Science and Technology, Shihezi University, Shihezi, Xinjiang 832003, China

ARTICLE INFO

Keywords:
Myofibrillar protein
Polyphenols
Interaction
Gel
Mechanism

ABSTRACT

The effects of four polyphenols—chlorogenic acid (CA), gallic acid (GA), epicatechin gallate (ECG), and epigallocatechin gallate (EGCG) on the structure, gel properties, and interaction mechanisms of myofibrillar protein (MP) were studied. The changes in MP structure with polyphenols were analyzed using circular dichroism. The ultraviolet and fluorescence spectra and thermodynamic analysis indicated that the type of binding between the four polyphenols with the MP was static quenching of complex formation. GA had a more pronounced effect on improving MP gel properties. Finally, molecular docking determined that the affinity of the protein with the four polyphenols was in the order EGCG > ECG > CA > GA, with the main interaction force being hydrophobic interactions and hydrogen bonding, but hydrogen bonding dominates the interaction between GA and the protein. The findings illuminate the mechanism of MP binding to different polyphenols and facilitate the study of polyphenol–protein properties.

1. Introduction

Myofibrillar proteins, as an essential component of muscle proteins (55–60 % of total muscle proteins), mainly include proteins such as myosin, actin, and troponin, which play a vital role in the textural properties of processed meat products (Hu, Gao, Solangi, Liu, & Zhu, 2022). Myosin, in particular, is the main cytoskeletal protein in myofibrils and the primary bearer of protein functional properties. Coregonus peled (*C. peled*) is a characteristic cold-water fish from Xinjiang, which has significant market potential in constructing high-quality protein products. However, during processing, temperature, pH, oxidation, and non-protein additives affect the performance and quality of protein products, of which oxidation is the most important and unavoidable.

Phenolic substances, derived from plant secondary metabolites, are widely present in foods such as fruits, vegetables, and grains, most of which have antioxidant and antimicrobial properties. These are often considered safe dietary sources of functional food additives, added to meat products mainly as antioxidants, such as tea polyphenols, apple polyphenols, mulberry polyphenols, etc. In recent years, phenolics bind with muscle proteins through reversible noncovalent and irreversible covalent interactions, and improving the protein functional properties has become a hot research topic. For example, the presence of sage extract made the MP emulsion interfacial film denser (Li, Liu, Liu, Kong, & Diao, 2019), kelp polyphenol extracts improved the gel properties of mackerel MP (He, Ming, Pu, Sun, Jin, Yu, et al., 2020), and mulberry polyphenols improved the digestibility and absorption properties of MP (Cheng, Tang, Yang, Wang, Lin, & Liu, 2023). However, various polyphenolic substances with complex systems exist in nature, in which phenolic acids and flavonoids are the most prevalent according to type. Tea contains a large number of polyphenols, of which epigallocatechin-3-gallate (EGCG) and epicatechin gallate (ECG) (belonging to flavonoids) are the majority of components. Yang and Cao et al. reported differences in the affinity of the complexes, changes in protein gel and emulsification properties, and antioxidant capacity when flavonoid components of tea interacted with MP (Yungang Cao, Ai, True, & Xiong, 2018; Yang, Zhao, Shan, Duan, Zhou, Cai, et al., 2023). Gallic acid (GA) and chlorogenic acid (CA) (belonging to phenolic acids) are also the main bioactive components of tea (Shang, Li, Zhou, Gan, & Li, 2021).

* Corresponding authors at: Food College, Shihezi University, North Fourth Road, Shihezi 832003, Xinjiang, China (J. Zhang).
E-mail addresses: wangzp@jiangnan.edu.cn (Z. Wang), zhangjian0411@163.com (J. Zhang).

https://doi.org/10.1016/j.fochx.2023.101063
Received 24 June 2023; Received in revised form 28 November 2023; Accepted 9 December 2023
Available online 12 December 2023

Pan and Zhou et al. reported the protein gel properties and glucose metabolism effects of phenolic acid polyphenols interacting with MP (Pan, Lian, Jia, Li, Hao, Wang, et al., 2020; Zhou, Wang, Xu, Dai, Lao, Zhang, et al., 2023). These findings provide a theoretical basis for the interaction of MP with polyphenols to enhance bioavailability and improve functional properties. However, there are strong and weak differences in the affinity of different polyphenols to interact with MP, and the polyphenol dose size leads to changes in the conformational and functional properties of the interaction with MP. In addition, further studies are needed to investigate the binding mechanisms, binding sites, and the effects of MP-polyphenol interactions on functional properties.

Therefore, in this paper, the four polyphenol monomers mentioned above (CA, GA, ECG and EGCG) were selected to interact with *C. peled* MP, respectively. According to the type and dose of different polyphenols, the MP-polyphenol complexes were investigated for the changes in conformation and gel properties, which provided another way to improve the gel properties of *C. peled* proteins. At the same time, the combination of multispectroscopy and molecular docking was used to explore the binding types and sites of MP-polyphenol interactions, laying the foundation for the subsequent investigation of the interaction mechanism between myosin and polyphenols in *C. peled*.

2. Materials and methods

2.1. Materials

C. peled was obtained from Saihu Fishery Technology Development Co. Ltd. (Xinjiang, China). Fresh *C. peled* were delivered to the laboratory via cold chain transportation. The dorsal muscles were sliced evenly, quickly frozen in liquid nitrogen, and stored at −80 °C in a refrigerator until needed. CA (purity ≥ 98 %), GA (purity ≥ 98.5 %), ECG (purity ≥ 98 %), and EGCG (purity ≥ 98 %) were purchased from YuanYe Biotechnology Co., Ltd. (Shanghai, China). All chemicals were analytical grade; distilled water was used for solution preparation and rinsing.

2.2. MP extraction

MP was extracted from *C. peled* using the previously described method (Zhang et al., 2021) with slight modification. Fish dorsal muscle was taken with pre-cooled distilled water (1:15, v:v) and homogenized in a meat grinder for 30 s. The mixture was centrifuged at 4 ℃ for 5 min at 5000 rpm to obtain the residue. The residue was stirred with 0.3 % NaCl (1:10, v:v) for 10 min with a magnetic stirrer, and the previous step of centrifugation was repeated to obtain the residue. The residue was then stirred with 8 times the volume of 20 mmol/L Tris-HCl (containing 0.6 mol/L NaCl, pH 7.0) with a magnetic stirrer at 4 °C for 1 h. The filtrate was obtained by filtration through 2 layers of gauze after the end of the reaction. The filtrate was diluted with 4 times the volume of pre-cooled distilled water, and the precipitate was obtained by centrifugation at 8000 rpm for 10 min at 4 °C, which was MP. Protein precipitates were solubilized with PBS (20 mmol/L phosphate buffer containing 0.6 mol/L NaCl, pH 7.0), and protein concentrations were tested by the Biuret method.

2.3. Incubation of MP and polyphenols

Polyphenol preparation is ready-to-use in capped centrifuge tubes (1.5 mL/5 mL). The volume of the polyphenol solution exceeds two-thirds of the total volume of the centrifuge tube. CA and GA (10 or 50 mmol/L) were prepared with 20 mmol/L phosphate buffer (pH 7.0), and ECG and EGCG (10 or 50 mmol/L) were prepared with 50 % ethanol solution. After preparing the polyphenol solution, it was protected from light with tin foil, stored in a refrigerator at 4 °C, and used within 10 min.

Proteins (10 mg/mL) were mixed well with different volumes of 10 mmol/L polyphenols (final polyphenol concentrations of 6, 30 and 150 μmol/g_{pro}, respectively), and PBS was added to homogenize the sample volume, which was dispensed in capped centrifuge tubes (the sample volume was greater than four-fifths of the total centrifuge tube volume). Incubate for 2 h at room temperature away from light for interaction. Samples without polyphenols and with the volume supplemented with PBS were considered controls. The complex was then diluted to the desired concentration to analyze and detect the physicochemical structural properties. Using proteins (50 mg/mL) interacting with polyphenols (50 mmol/L) to prepare complex as similarly described. End of incubation, the protein concentration was adjusted to 40 mg/mL with PBS for preparing gels. In particular, the protein–polyphenol interaction was studied by fluorescence quenching in a dilute solution, as described in Methods 2.7.

2.4. Sulfhydryl (-SH) content and free amino group levels

According to the method of Hu et al. (Hu, Gao, Solangi, Liu, & Zhu, 2022), the SH group content was determined using 2,2′-dinitro-5,5′-dithiobenzoic acid (DTNB), expressed as nmol sulfhydryl/mg protein. Briefly, samples were mixed with 50 mmol/L sodium phosphate buffer (0.6 mol/L KCl, 10 mmol/L EDTA, and 8 mol/L urea, at pH 7.0) and DTNB. The absorbance was measured at 412 nm after being reacted at 40 °C for 25 min.

According to the method of Hu, Gao, Solangi, Liu, and Zhu (2022), 80 mg of o-phthalaldehyde (OPA) was dissolved in ethanol, 1 mL of 10 % sodium dodecyl sulfate (SDS) and 200 μL of 2-mercaptoethanol were added sequentially, and sodium borate buffer solution (0.1 mol/L, pH 9.75) was added to a constant volume of 100 mL. After 4 mL OPA reagent and 200 μL protein sample were mixed thoroughly, they were reacted at 37 °C for 3 min in the dark. Absorbance was recorded at 340 nm, and free amino equivalent was calculated. A standard curve was prepared with glycine (0–10 mmol/L).

2.5. Surface hydrophobicity (S_0)

Surface hydrophobicity was determined using 1-anilinonaphthalene-8-sulfonic acid (ANS), according to Pessato et al. (Pessato et al., 2016) with slight modifications. The protein concentration (2 mg/mL) was diluted to 0.05–0.2 mg/mL, and 20 μL of 8 mmol/L ANS (dissolved in 10 mmol/L phosphate buffer, pH 7.0) was mixed with a 4 mL protein sample. Then the mixture was kept in the dark for 2 min. The fluorescence intensity was recorded with a fluorescence spectrometer (970 CRT, Shanghai Precision Instrument Co., Ltd., Shanghai, China) at an excitation wavelength of 390 nm and an emission wavelength of 470 nm.

2.6. Circular dichroism (CD) spectroscopy

According to Liu, Zhang, Guo, Zhu, Mao, Guo, et al. (2021), the CD spectrum from 195 to 240 nm at 298 K was determined through a 1 mm path-length quartz cell using a circular dichroism spectrometer (MOS-450, Biologic, Rennes, France). The sample solution was diluted to 0.2 mg/mL with PBS. DichroWeb was used to analyze the contents of secondary structures of samples, and the data are given as mean residue ellipticity.

2.7. UV–vis absorption spectra and fluorescence spectroscopy

The protein samples were scanned for UV spectra at 200–700 nm using a UV spectrophotometer (T3200, Youke Instrument Co., Ltd., Shanghai, China). Synchronous fluorescence spectra were recorded in the range of 280–400 nm (Δ λ = 15 nm; Δλ = 60 nm) at 298 K. The protein samples were scanned using a fluorescence spectrometer. Polyphenols were added to the protein solution (0.4 mg/mL) and mixed well. The mixture was placed in a water bath at 25, 35, and 45 °C for 2 min,

and the fluorescence spectrum at 300–450 nm under excitation at 280 nm was recorded using a spectrofluorometer.

2.7.1. Fluorescence data analysis

The Stern–Volmer equation is used to discriminate the fluorescence quenching mechanism, including dynamic and static quenching. It is calculated using the following formula:

$$F_0/\ F = 1 + K_q \times \tau_0 \times [Q] = 1 + K_{sv} \times [Q] \quad (1)$$

where F_0 is the initial fluorescence intensity, F is the fluorescence intensity of the added quencher, K_q is the quenching rate constant, τ_0 is the average fluorescence lifetime of the biomolecule without any quencher ($\tau_0 = 10^{-8}$ s), K_{sv} is the quenching constant, and [Q] is the concentration of the quencher. When $K_q > 2.0 \times 10^{10}$ L/(mol·s), the quenching mode is static; otherwise, it is dynamic. For static quenching, the double logarithmic equation can calculate the binding constant (K_A) and the number of binding sites (n). The equation is as follows:

$$Lg = Lg \times K_a + n \times Lg\ [Q] \quad (2)$$

2.7.2. Thermodynamics research

The thermodynamic parameters related to the binding process of protein and polyphenols were calculated by the van't Hoff equation (Abdur, 2021). The thermodynamic parameters enthalpy change (ΔH), entropy change (ΔS), and Gibbs free energy change (ΔG) at corresponding temperatures (25, 35, 45 °C) were obtained. The formula is as follows:

$$\ln\ K_a = -\Delta H/(R \times T) + \Delta S\ /\ R \quad (3)$$

$$\Delta G = \Delta H - T \times \Delta S = -R \times T \times \ln\ K_a \quad (4)$$

where T (K) is the absolute temperature, K_a is the binding constant at relative temperature, and R is the gas constant (R = 8.314 J/(mol × K)). These calculations determined the main types of forces in the protein–polyphenol system.

2.8. Gelling properties of MP

2.8.1. Cooking loss, gel strength, and water holding capacity (WHC)

Protein–polyphenol samples (40 mg/mL) were centrifuged at 1000*g* for 2 min to remove air bubbles. The samples were poured into lidded glass jars and preheated in a water bath at 40 °C for 2 h, then heated from 40 to 95 °C at 1 °C/min and held for 30 min. After heating, the glass jars were cooled in ice water for 10 min. Finally, the gels were stored in a refrigerator for 12 h. The samples were allowed to equilibrate at room temperature (25 °C) for 2 h before the analytical tests.

Cooking loss is a measure of the weight of drained liquid from the sample after heating as a percentage of the weight of the sample before heating. The TA-XT Plus Texture Analyzer (Stable Micro Systems Ltd., Surrey, UK) was used to measure the gel strength with a probe (P/0.5). The measurement parameters were as follows: pre-speed with 2.00 mm/s; test speed with 1.00 mm/s; post-speed with 1.00 mm/s; and trigger force with 5 g. The gel was placed in a centrifuge tube and weighed, then centrifuged at 3000*g* for 15 min to remove the water and re-weighed. WHC was presented as the final weight ratio to the initial weight.

2.8.2. Microstructure of gels

The microstructure of the gel samples was observed with a scanning electron microscope (SU8010, Hitachi, Japan). The gel samples were cut (5 × 5 × 5 mm^3) and then fixed in 2.5 % glutaraldehyde for 24 h. Gradient dehydration was carried out with 30, 40, 50, 60, 70, 80, 90, 95, and 100 % ethanol. After freeze-drying and gold spraying, the samples were magnified 1000 times for observation.

2.9. Protein homology modeling and molecular docking

2.9.1. Protein homology modeling

The crystal structure of *C. peled* MP has not been available in the Uniprot (https://www.uniprot.org/) and NCBI (https://www.ncbi.nlm.nih.gov/) databases. As the major protein in MP (55–60 %), myosin was used as the next target for modeling and molecular docking studies. Meanwhile, the Uniprot database reports similar homologs of the myosin heavy chain (MHC) crystal structure of *Coregonus* spp.

The extracted MP was subjected to SDS–polyacrylamide gel electrophoresis (SDS PAGE). In short, protein samples were diluted to 6 mg/mL with PBS and then diluted with 2× sampling buffer (0.5 mol/L Tris-HCl pH 6.8, glycerol, 20 % SDS, 0.1 % bromophenol blue, water, and β-mercaptoethanol), followed by heating of the samples at 95 °C for 10 min. SDS-PAGE gels were prepared from 5 % stacking and 12 % separating gel. The samples were uploaded at 12 μg, and the stacking and separating gel were run with 80 V and 160 V currents, respectively. After electrophoresis, the gel was stained with staining solution (0.25 % Coomassie brilliant blue G-250, 50 % methanol, 10 % acetic acid glacial) for 40 min and then repeatedly decolorized with decolorizing solution (25 % methanol, 7.5 % acetic acid glacial) until the gel was transparent.

The gum strips were excised from the heavy chain of myosin and identified by high-performance liquid chromatography–tandem mass spectrometry (HPLC-MS/MS), using a RIGOL L-3000 high-performance liquid chromatography system (Beijing Puyuan Jingdian Technology Co., China) and an Orbitrap Eclipse mass spectrometer according to Ma et al., with slight modifications (Wang et al., 2021). The gum strips were trypsinized and freeze-dried. The samples were then desalted and washed with a C18 desalting column to remove impurities and eluted with 70 % acetonitrile and freeze-dried to obtain solid samples. Mobile phases consisted of liquid A (100 % water, 0.1 % formic acid) and liquid B (80 % acetonitrile, 0.1 % formic acid). The full scan range of mass spectrometry was 350–2000 *m/z*. The elution conditions were as follows: 6 % B to 30 % B (0–46 min), 30 % B to 40 % B (46–53 min), and 40 % B to 95 % (53–64 min). Proteome Discoverer 2.4 software and the Uniprot database were used to search and identify the proteins with the highest scores and broadest coverage. The protein sequence of MHC was obtained from the Uniprot database (primary accession: A0A6F9C6S1). Homology modeling was completed through the SWISS-MODEL website (https://swissmodel.expasy.org/), and the protein model was evaluated using the SAVES 6.0 website (https://servicesn.mbi.ucla.edu/).

2.9.2. Molecular docking

The molecular docking of myosin and polyphenols was studied using AutoDock Vina software. Pretreatment of the myosin model (dehydration, hydrogenation, and charge) was achieved using AutoDock Tools 1.5.7. The molecular and 3D structures of CA, GA, ECG, and EGCG were downloaded from the PubChem database (https://pubchem.ncbi.nlm.nih.gov/) and obtained using Chem3D software energy minimization with the MM2 force field. The minimum binding energy and corresponding binding configurations were obtained from the AutoDock Vina scoring function.

2.10. Statistical analysis

The experiment was independently repeated 3 times with fresh samples prepared from different batches, and the data are presented as mean ± standard deviation (SD). ANOVA was performed by SPSS 25.0 to consider the level of significance ($P < 0.05$) between means. Origin 8.5 was used to make the graph, Pymol was used for the 3D mapping of molecular docking, and LigPlus was used for the 2D mapping of docking.

Table 1
Changes in physicochemical and gel properties of the MP-polyphenol.

MP-polyphenol	Total sulfhydryl (nmol/mg protein)	Free amino group (nmol/mg protein)	Surface hydrophobicity	Cooking loss (%)	Gel strength (g)	Water holding capacity (%)
Control	69.90 ± 0.07^{a}	230.90 ± 8.63^{a}	71.99 ± 0.69^{a}	11.86 ± 0.27^{f}	32.42 ± 1.59^{f}	52.40 ± 0.14^{d}
MP-CA_6	67.81 ± 0.42^{a}	216.74 ± 4.06^{b}	70.77 ± 0.85^{a}	13.04 ± 1.23^{f}	41.75 ± 1.84^{e}	52.46 ± 1.81^{d}
MP-CA_{30}	65.18 ± 0.42^{b}	191.51 ± 0.77^{d}	66.64 ± 0.96^{ab}	11.86 ± 0.10^{f}	59.45 ± 3.61^{e}	46.93 ± 1.69^{d}
MP-CA_{150}	56.08 ± 0.12^{c}	179.56 ± 3.34^{e}	52.92 ± 0.91^{de}	34.42 ± 2.95^{d}	168.10 ± 14.97^{d}	46.89 ± 5.23^{c}
MP-GA_6	65.78 ± 0.29^{b}	198.59 ± 0.89^{c}	71.45 ± 1.84^{a}	13.50 ± 1.02^{f}	50.21 ± 3.47^{e}	50.71 ± 0.94^{d}
MP-GA_{30}	58.17 ± 0.18^{c}	192.39 ± 2.30^{d}	66.99 ± 0.63^{ab}	13.12 ± 0.13^{f}	53.62 ± 2.55^{e}	50.40 ± 2.58^{d}
MP-GA_{150}	29.64 ± 0.20^{f}	168.49 ± 1.33^{ef}	56.00 ± 1.52^{d}	20.12 ± 1.89^{e}	122.55 ± 7.23^{d}	64.69 ± 4.88^{d}
MP-ECG_6	67.33 ± 0.12^{a}	191.07 ± 2.03^{d}	61.88 ± 0.40^{bc}	12.00 ± 0.77^{f}	54.83 ± 3.38^{e}	49.84 ± 2.08^{d}
MP-ECG_{30}	54.17 ± 0.07^{d}	164.07 ± 1.17^{f}	61.17 ± 1.13^{c}	64.56 ± 3.02^{c}	368.02 ± 13.96^{c}	79.78 ± 4.58^{b}
MP-ECG_{150}	24.04 ± 0.29^{fg}	139.28 ± 1.33^{g}	34.11 ± 0.60^{f}	74.06 ± 4.00^{b}	1172.38 ± 30.97^{a}	89.03 ± 5.13^{a}
MP-$EGCG_6$	66.46 ± 0.71^{ab}	192.39 ± 2.66^{d}	64.07 ± 2.33^{b}	12.18 ± 0.54^{f}	52.76 ± 1.15^{e}	50.40 ± 2.76^{d}
MP-$EGCG_{30}$	44.35 ± 1.63^{e}	174.25 ± 4.27^{e}	56.31 ± 1.08^{d}	62.94 ± 3.48^{c}	478.26 ± 17.39^{b}	68.82 ± 0.95^{c}
MP-$EGCG_{150}$	13.35 ± 1.14^{h}	115.38 ± 5.79^{h}	20.41 ± 0.62^{g}	81.04 ± 4.01^{a}	1011.30 ± 12.86^{a}	86.65 ± 3.65^{a}

Results are presented as mean ± standard deviation. Columns with different letters (a-h) indicate a significant difference ($P < 0.05$) according to Duncan's multiple range test.

3. Results and discussion

3.1. Sulfhydryl (-SH) and the free amino group ($-NH_2$)

The total sulfhydryl content can reflect the changes in protein amino acid side chain groups. As shown in Table 1, adding polyphenols reduced protein -SH, which showed a dose-dependent downward trend. The -SH value decreased with increased polyphenol concentration after adding polyphenols compared with the control. Four polyphenols at a dose of 6 μmol/g_{pro} did not significantly affect the loss of -SH ($P > 0.05$). In contrast, EGCG added at the same dose showed a more remarkable ability to deplete thiol groups than the others, and the order of -SH consumption was: EGCG > ECG > GA > CA. Similar to the results of this paper, the reaction of pea isolates with 25–250 μmol/g of CA, EGCG and RES (resveratrol) all resulted in a significant decrease in protein-SH content (Hao, Sun, Pei, Zhang, Li, Li, et al., 2022). Cao and Xiong (2017) claimed that under polyphenol and neutral pH conditions, sulfhydryl groups tend to deprotonate, and the formed sulfhydryl ions react

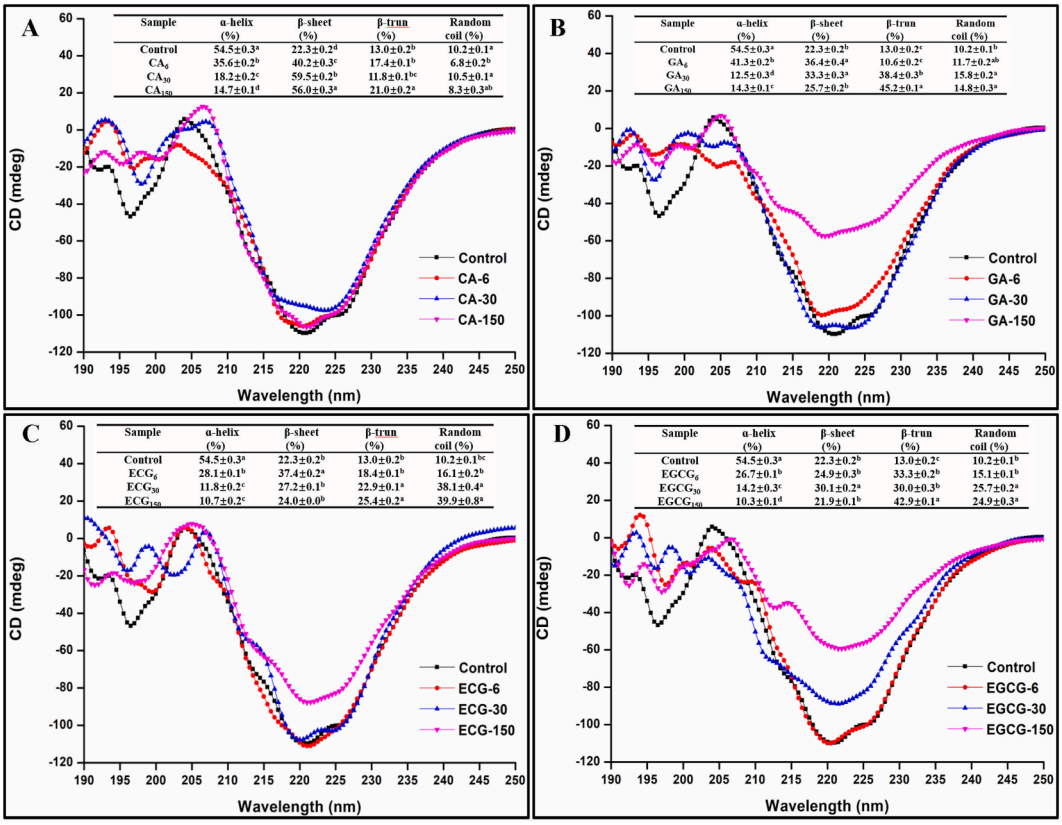

Fig. 1. Circular dichroism (CD) spectroscopy of MP-CA (A), MP-GA (B), MP-ECG (C), and MP-EGCG (D); the inserted table presents the percentage distribution secondary structure of MP-CA/GA/ECG/EGCG. Note: The different letters represent a significant difference between samples ($p < 0.05$); MP, myofibrillar protein; CA, chlorogenic acid; GA, gallic acid; ECG, epicatechin gallate; EGCG, epigallocatechin gallate.

with the carbonyl group to reduce the sulfhydryl content. What's more, the hydroxyl groups of polyphenols can interact with protein sulfhydryl groups to reduce -SH content (Sui et al., 2018). Polyphenols with different molecular weights and structures affect the interaction with proteins (Frazier et al., 2010), which may be the reason why MP sulfhydryl groups are consumed differently by adding the four polyphenols. EGCG has more phenolic hydroxyl groups than the other three polyphenols, which makes it more likely to interact with sulfhydryl groups. Moreover, EGCG is susceptible to autoxidation in neutral and alkaline environments to form o-quinone, which covalently binds to protein-SH and significantly depletes the -SH content (Wei, Chen, Ling, Wang, Dong, Zhang, et al., 2016).

Adding four polyphenols resulted in the loss of protein-NH_2, and the intensity of loss was EGCG > ECG > GA > CA. This is similar to the trend of sulfhydryl depletion. This is similar to the trend of sulfhydryl depletion, in which is possible that the interaction between (examples include the oxidation of polyphenol hydroxyl groups to quinone to form C—N bonds with $–NH_2$, interactions between hydroxyl groups of polyphenols and amino acid nitrogen and oxygen, and hydrophobic interactions between polyphenols and amino acids) the protein and the polyphenols leads to a decrease in the highly reactive $–NH_2$ groups. Similar results were reported by Yan, Wang, Yu, Li, and Qi (2023).

3.2. Surface hydrophobicity (S_0)

The exogenous ANS fluorescence probe can reflect the surface exposure of hydrophobic sites and protein conformational changes. Table 1 shows that the hydrophobicity of the protein surface decreased after the polyphenols were added compared with the control ($P < 0.05$). Notably, with CA, GA, ECG, and EGCG at 150 μmol/g_{pro}, the surface hydrophobicity decreased sharply by 26.49, 22.21, 52.62, and 71.65 %, respectively, suggesting that EGCG has a more substantial polar effect than the other three. Polyphenols contain multiple hydroxyl groups, and when bound to proteins, bringing in additional hydroxyl groups increases the hydrophilic environment of the protein, hinders the excitation of ANS, and reduces its fluorescence intensity. At the same time, polyphenols compete with the ANS fluorescence probe for hydrophobic groups on the protein's surface to reduce the binding site between the protein and the ANS (Cao, Xiong, Cao, & True, 2018). This result is similar to the reduced surface hydrophobicity of soy protein, casein, and whey protein isolate after adding phenolic compounds (Jiang, Zhang, Zhao, & Liu, 2018). Moreover, compared with CA and GA, ECG and EGCG have multiple benzene rings and hydroxyl groups. This result was similar to that of Hao et al., who reported that EGCG had a more significant ability to reduce surface hydrophobicity than chlorogenic acid and resveratrol (Hao et al., 2022). The structural diversity may be the main reason why ECG and EGCG significantly reduced the surface hydrophobicity, which echoes the results mentioned above.

3.3. Circular dichroism (CD) spectroscopy

Circular dichroism (CD) can reflect changes in protein secondary structure. Fig. 1 shows that adding polyphenols increased protein ellipticity, indicating a change in protein secondary structure. When polyphenols were added, the β-sheet increased with the reduction in the α-helix. Compared with the control, adding 150 μmol/g_{pro} of CA, GA, ECG, and EGCG reduced the α-helix content by 73.03, 73.76, 80.37, and 81.10 %, respectively. These results were mainly attributed to the

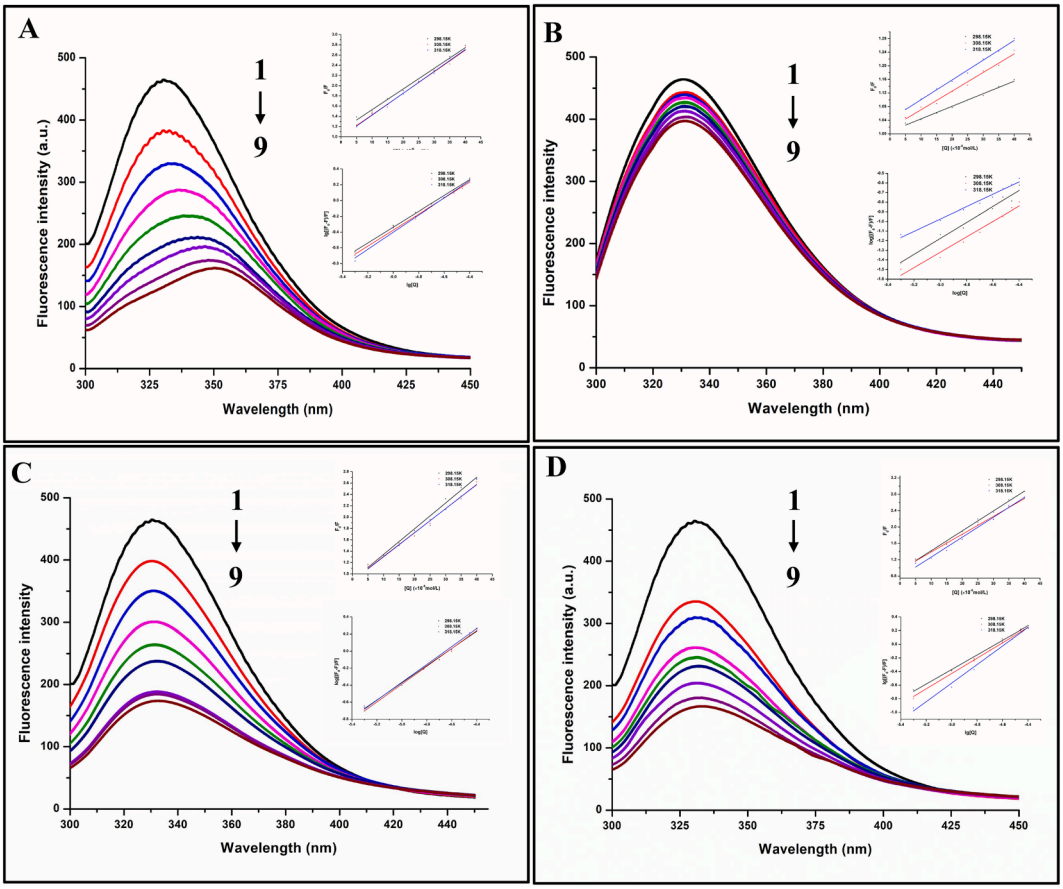

Fig. 2. Fluorescence spectra of MP MP-CA (A), MP-GA (B), MP-ECG (C), and MP-EGCG (D)0.1–9: MP with 0, 5, 10, 15, 20, 25, 30, 35, 40 μmol/g_{pro} of CA, GA, ECG, and EGCG. The inset graph shows the Stern-Volmer equation of MP fluorescence quenching in the presence of CA (A), GA (B), ECG (C), and EGCG (D) at 25 °C, 35 °C, and 45 °C. Note: MP, myofibrillar protein; CA, chlorogenic acid; GA, gallic acid; ECG, epicatechin gallate; EGCG, epigallocatechin gallate.

Table 2
Quenching rate constants constant (K_q), binding constant (K_a), binding site number (n), and thermodynamic parameters for MP interactions with CA, GA, ECG, and EGCG at different temperatures.

MP-polyphenol	T(K)	K_q ($\times 10^{12}$ L mol^{-1} s^{-1})	K_a ($\times 10^4$ L/mol)	n	ΔG (K J/mol)	ΔH(K J/mol)	ΔS (J mol^{-1} K^{-1})	R^2
MP-CA	298.15	4.159 ± 0.04^{cd}	4.780 ± 0.29^{d}	1.00 ± 0.01	−26.71 ± 0.12^{b}	3.24 ± 0.01^{c}	100.44 ± 2.09^{b}	0.9767
	308.15	4.025 ± 0.03^{d}	4.987 ± 0.33^{d}	1.01 ± 0.01	−27.71 ± 0.20^{b}			0.9855
	318.15	3.485 ± 0.02^{e}	10.688 ± 1.20^{b}	1.08 ± 0.02	−30.63 ± 0.20^{a}			0.9978
MP-GA	298.15	0.698 ± 0.01^{f}	0.093 ± 0.01^{e}	0.83 ± 0.02	−16.96 ± 0.36^{d}	−50.95 ± 0.03^{c}	−114.01 ± 3.00^{c}	0.9709
	308.15	0.668 ± 0.01^{f}	0.048 ± 0.02^{e}	0.80 ± 0.01	−15.82 ± 0.65^{cd}			0.9677
	318.15	0.427 ± 0.02^{g}	0.017 ± 0.02^{e}	0.64 ± 0.01	−13.61 ± 0.23^{c}			0.9798
MP-ECG	298.15	4.460 ± 0.03^{b}	4.720 ± 0.66^{d}	1.01 ± 0.02	−26.68 ± 0.24^{bc}	31.13 ± 0.10^{b}	193.90 ± 2.94^{a}	0.9974
	308.15	4.271 ± 0.02^{bc}	7.095 ± 1.01^{c}	1.05 ± 0.01	−28.62 ± 0.20^{ab}			0.9963
	318.15	4.222 ± 0.04^{c}	7.790 ± 1.35^{c}	1.05 ± 0.01	−29.79 ± 0.38^{ab}			0.9850
MP-EGCG	298.15	5.049 ± 0.08^{a}	9.359 ± 2.09^{b}	1.07 ± 0.02	−28.37 ± 0.21^{b}	40.47 ± 0.33^{a}	230.90 ± 4.21^{a}	0.9964
	308.15	4.430 ± 0.05^{b}	15.897 ± 2.27^{a}	1.13 ± 0.02	−30.68 ± 0.20^{a}			0.9911
	318.15	4.161 ± 0.04^{cd}	17.444 ± 1.58^{a}	1.36 ± 0.03	−31.92 ± 0.33^{a}			0.9902

MP, myofibrillar protein; CA, chlorogenic acid; GA, gallic acid; ECG, epicatechin gallate; EGCG, epigallocatechin gallate. Results are presented as mean ± standard deviation. Columns with different letters (a-f) indicate a significant difference ($P < 0.05$) according to Duncan's multiple range test.

binding of proteins to polyphenols promoting protein conformational changes. The multiple hydroxyl groups of polyphenols may break the intermolecular hydrogen bonds in the stable helices, which decompose and unwind (Taotao et al., 2019). In addition, the random coil content also increased with the addition of polyphenols, implying a transition from order to disorder in the protein structure.

3.4. UV–Vis absorption spectra

The interaction of proteins with small molecule compounds can be analyzed by UV–Vis absorption spectroscopy. Fig. S1 shows the UV–Vis spectra of MP combined with the four polyphenols. Due to the presence of tryptophan, tyrosine, and phenylalanine, myofibrillar protein had a prominent absorption peak near 280 nm. The addition of polyphenols increased the absorption value of the protein at 280 nm, indicating that the aromatic amino acids buried inside the protein were exposed. In other words, the protein modification of the microenvironment or structure changed upon binding with the polyphenols. Meanwhile, a significant red shift (from 277.5 to 284.8 nm) in the presence of CA near the absorption peak at 280 nm and a blue shift to varying degrees in the presence of GA and EGCG (GA: 277.5 to 259.9 nm; EGCG: 277.5 to 274.7 nm) occurred, indicating that the polarity of the protein was altered when the polyphenol was bound to it (Khan, Zafar, & Naseem, 2019). Notably, a new absorption peak was generated with CA at a dose of 150 μmol/g_{pro}, which may be attributed to the different types of polyphenols. Similar to the results of this experiment, a new peak of the β-lactoglobulin-CA system at 342 nm was also observed (Xu et al., 2019). In addition, the fluorescence quenching mechanism of MP-CA/GA/ECG/EGCG can also be presumed from the above results. Because dynamic quenching only affects the excited state of fluorescent molecules, without changing the absorption spectrum, static quenching would also change the absorption spectrum of fluorescent molecules due to the formation of complexes. Accordingly, it can be deduced that the quenching mechanism between MP-CA/GA/ECG/EGCG is static quenching.

3.5. Synchronous fluorescence spectra

Synchronous fluorescence spectra can reflect changes in the microenvironment of a single chromophore when proteins interact with polyphenols (Zahirović, et al., 2019). Fig. S2 shows that the fluorescence intensity of tryptophan (Trp) and tyrosine (Tyr) was reduced with increasing polyphenol. The interaction of the protein with CA resulted in a minor red shift of the Trp spectrum and a slight blue shift of the Tyr spectrum. The spectra of both Trp and Tyr were slightly red-shifted when interacting with GA, ECG, and EGCG, indicating that the existence of polyphenols created protein changes in the hydrophobicity. These results were attributed to differences in protein conformation by the interaction of polyphenols with proteins. In addition, the fluorescence intensity of Trp was significantly higher than that of Tyr, indicating that the fluorescence of MP was mainly derived from Trp.

The ratio of simultaneous fluorescence quenching ($RSFQ = 1 - F/F_0$) can determine which amino acid residue is closer to the ligand (He Zhiyong, Xu Mingzhu, Zeng Maomao, Qin Fang & Chen Jie, 2016). Table S1 shows that the RSFQ values at $\Delta\lambda = 60$ nm for GA/ECG/EGCG were more significant than those at $\Delta\lambda = 15$ nm in the same concentrations, indicating that the binding sites of these three polyphenols to the proteins were closer to the Trp residues. However, the RSFQ values for CA at $\Delta\lambda = 60$ nm were all smaller than the RSFQ values at $\Delta\lambda = 15$ nm, indicating that the binding sites of CA to the protein were closer to the Tyr residues.

3.6. Fluorescence quenching mechanism and binding constant

Proteins have endogenous fluorescence due to chromophores such as tryptophan, tyrosine, and phenylalanine. Fluorescence quenching can reflect the interactions between proteins and biologically active molecules (Patil, Sandberg, Heckert, Self, & Seal, 2007). Changes in the endogenous fluorescence spectra of proteins with different concentrations of the four polyphenols were measured at three temperatures. Fig. 2 shows that the protein had a maximum emission wavelength of 330 nm. The protein fluorescence intensity decreased significantly when polyphenols were added at increased concentrations, suggesting that the polyphenols quenched the protein fluorescence intensity in a concentration-dependent manner. In addition, CA caused a red shift of the maximum emission wavelength from protein, implying a transition from hydrophobicity to hydrophilicity in the internal environment of the amino acid residues.

To clarify the quenching mechanism, Stern–Volmer curves of MP-CA/GA/ECG/EGCG were drawn, as shown in Fig. 2. Applying the Stern–Volmer equation, the curve of F_0/F versus polyphenol concentration shows good linearity ($r^2 > 0.9$). The K_q values (0.427–5.049 × 10^{12} L/mol/s) are more significant than the maximal dynamic quenching constant (2.0 × 10^{10} L/mol/s), implying the formation of complexes between fluorescent groups and quenchers, that is, static quenching (Moeiniafshari, Zarrabi, & Bordbar, 2015). Similar results were reported for the noncovalent binding of whey proteins and chlorogenic acid with phenolic derivatives (EGCG) in scallop gonad protein isolates (Zhang et al., 2021;Han et al., 2021).

The binding constant (K_a) and binding site number (n) in Table 2 were obtained by analyzing static quenching data using a double logarithmic curve equation. In our study, the n values of three temperatures were close to 1, which indicates that there might be a single binding site on MP for phenolics. Values larger than 10^4 L mol^{-1} for K_a indicate a high affinity for polyphenols. Therefore, the affinity between the four polyphenols and MP is as follows: K_a (EGCG) > K_a (ECG), K_a (CA) > K_a

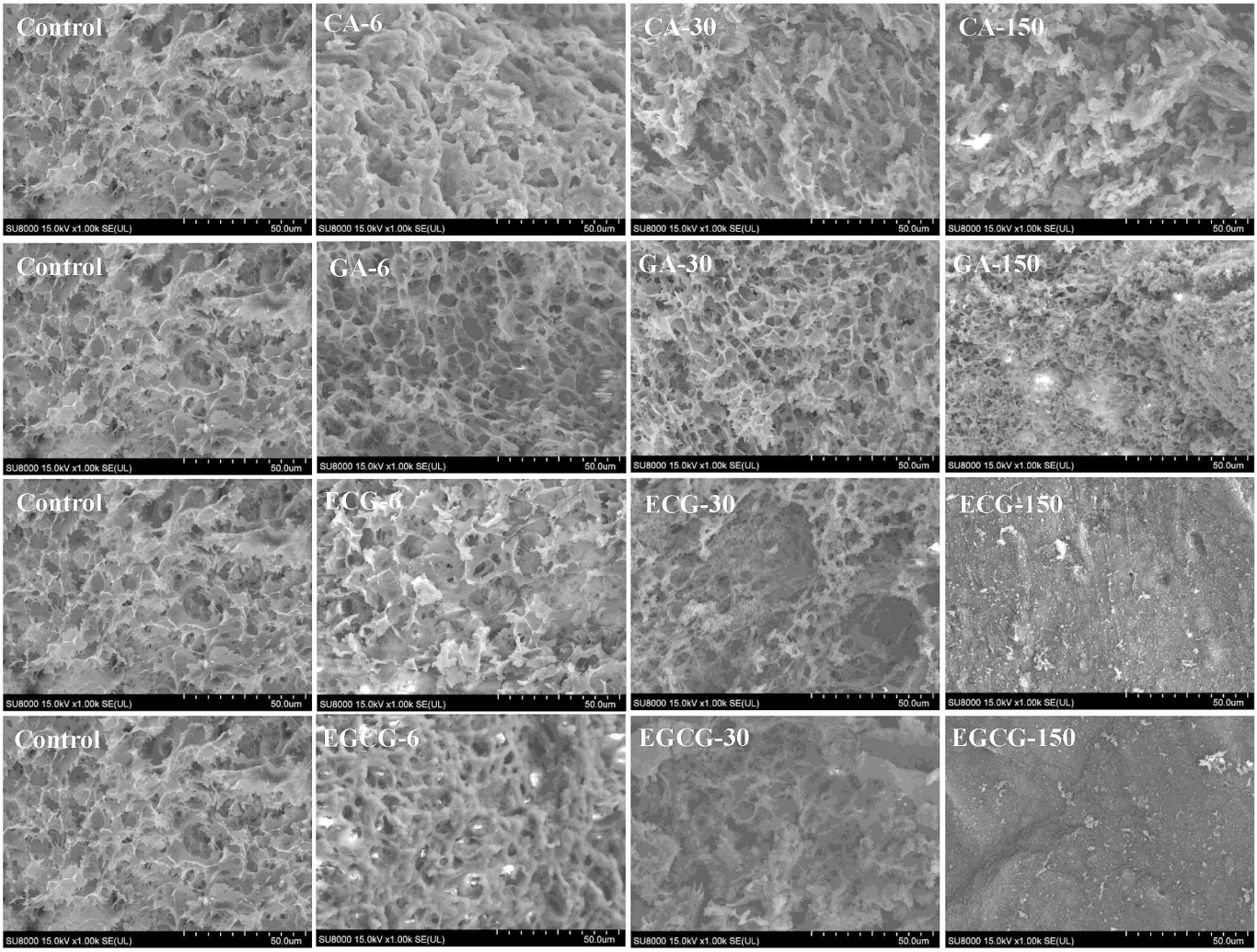

Fig. 3. Scanning Electron Microscope of MP-CA, MP-GA, MP-ECG, and MP-EGCG. MP, myofibrillar protein; CA, chlorogenic acid; GA, gallic acid; ECG, epicatechin gallate; EGCG, epigallocatechin gallate.

(GA). Furthermore, K_a increased as a function of temperature, revealing that the formation of MP-CA, MP-ECG, and MP-EGCG complexes became more favorable, and the complex stability increased, a characteristic feature of hydrophobic interactions (Zeng, Zhang, Lin, Gong, & Chemistry, 2016). There is a correspondence to the following thermodynamic parameter results. The number of hydroxyl groups contained in polyphenols and their molecular structure play vital roles in binding phenolic substances to proteins. From the perspective of polyphenol molecular conformation, the probability that EGCG molecule will bind with protein space is more remarkable because the spatial structure of EGCG is larger, and more –OH groups are associated with it (Hasni et al., 2011). Moreover, changes in the dominance of interaction forces between protein and polyphenol may also affect the binding force under the influence of temperature (Joye, Davidov-Pardo, Ludescher, & McClements, 2015).

3.7. Thermodynamic analysis of MP–polyphenol interactions

Thermodynamic parameters, including ΔG, ΔS, and ΔH, are mainly used to analyze noncovalent driving forces between small molecule substances and proteins. Table 2 shows that ΔG was negative under the three temperatures, indicating that the interaction of polyphenols with MP was a spontaneous reaction driven by Gibbs free energy. When $\Delta H > 0$ and $\Delta S > 0$, the primary binding force is a hydrophobic interaction; when $\Delta H < 0$ and $\Delta S > 0$, the electrostatic interaction is the main force; and when $\Delta H < 0$ and $\Delta S < 0$, the van der Waals force and hydrogen bonding are the main forces (Ross & Subramanian, 1980). In our results, the binding of MP-CA, MP-ECG, and MP-EGCG was mainly based on hydrophobic interaction, while the MP–GA combination was primarily due to hydrogen bonds and van der Waals force. Many studies have shown that polyphenols and proteins are bound mainly by hydrophobic interactions, hydrogen bonds, and van der Waals force (Bhimaneni, Bhati, Bhosale, & Kumar, 2021). Hydrogen bonding interactions between proteins and polyphenols are also possible due to the presence of hydroxyl groups. Previous scholars found that the interaction forces between pea protein (PPI) and EGCG are hydrogen bonding and van der Waals force, but the force between PPI and CA is mainly electrostatic interaction (Hao et al., 2022). The inconsistency in this paper may be attributed to the complex structure of different proteins.

3.8. Cooking loss, gel strength, and water holding capacity (WHC)

Fig. S3 shows comparisons of polyphenol–MP solution and polyphenol–protein gels. It can be observed that the ECG and EGCG at 30 and 150 μmol/g_{pro} prompted aggregation of the solution and the appearance of flocculent material. After heating, adding ECG and EGCG at this dose significantly reduced the protein gel yield. Moreover, the involvement of polyphenols improved the MP gel properties to some extent.

Table 1 shows the effect of polyphenols on MP gel. Adding 6 μmol/g_{pro} polyphenols had no significant impact on the gel cooking loss ($P >$

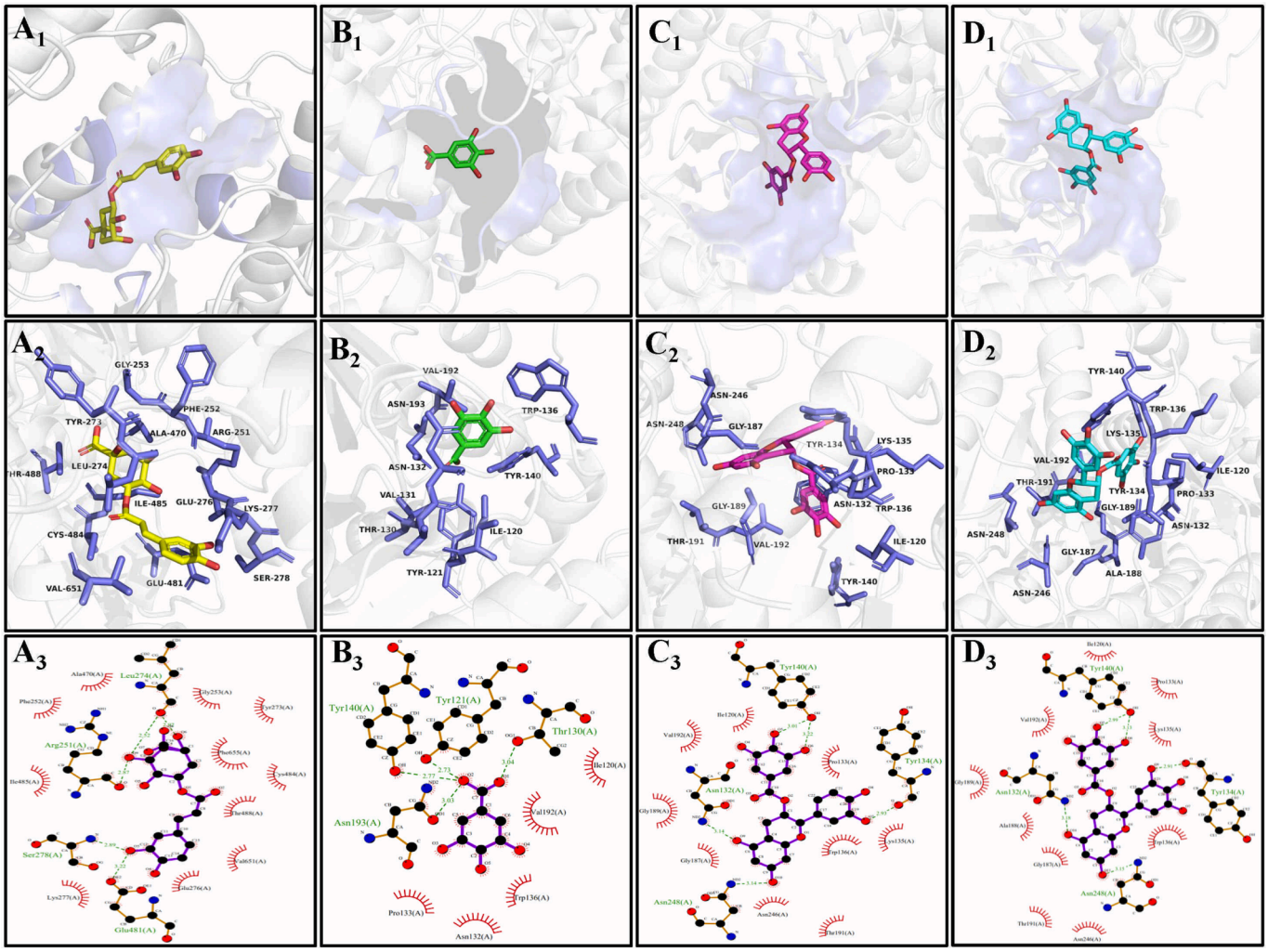

Fig. 4. Interaction analysis between myosin and polyphenols. 3D docking mode between myosin and CA (A_1), GA (B_1), ECG (C_1), EGCG (D_1); the detailed (3D) binding mode of the myosin complex (distance < 5 Å; CA (A_2), GA (B_2), ECG (C_2), EGCG (D_2)); 2D schematic interaction diagram between myosin and CA (A_3), GA (B_3), ECG (C_3), EGCG (D_3). Note: CA, chlorogenic acid; GA, gallic acid; ECG, epicatechin gallate; EGCG, epigallocatechin gallate.

0.05). The gel cooking loss increased as the dose of polyphenols increased ($P < 0.05$). Especially for ECG and EGCG, the cooking loss increased to 74.06 and 81.04 % when the amount of polyphenol reached 150 μmol/g_{pro}, severely reducing the gel yield. Wang et al. reported that 50–100 μmol/g neomethyl hesperidin dihydrochalcone (NHDC) caused protein aggregation, affected protein cross-linking, and increased cooking losses (Wang et al., 2022). Similarly, protein gel WHC increased sharply with the addition of ECG and EGCG (over 6 μmol/g_{pro}), as shown in Table 1. ECG and EGCG lost significant water during the cooking process. The high WHC in this result mainly occurred because excessive polyphenols can aggregate protein, resulting in gels that can no longer trap water. The MP gel strength is shown in Table 1. The MP gel without polyphenols was weaker, and the gel collapse can be observed in Fig. S3. MP gel strength increased significantly when adding polyphenols ($P < 0.05$). However, excessive gel strength resulted in "agglomerates" when the ECG or EGCG concentration was over 6 μmol/g_{pro}. This may be due to the attachment of excess polyphenols to the protein surface, which has a substantial hydrophobic effect by shielding the protein reactive functional groups (–SH and $–NH_3$), contributing to the aggregation of proteins and hindering protein interactions, thus disrupting the formation of the protein gel network structure (Cao & Xiong, 2015). In contrast, adding GA at 150 μmol/g_{pro} promoted protein gel WHC. Analyzed from an interaction perspective, the MP–GA interaction was dominated by hydrogen bonding, which slowed down the cross-linking between shielding proteins caused by hydrophobic interactions and enhanced the noncovalent chemical forces of the polyphenol–protein gels. In addition, hydrogen bonding facilitates the capture of more water during protein gelation (Wang et al., 2022). Therefore, cross-linked aggregation between GA and MP improved protein gel performance.

3.9. Microstructure of gels

Fig. 3 shows the microstructure of the protein gel. The control had a typical gel network structure, but the gel pore size was lamellar and inhomogeneous. After adding polyphenols, the protein gel network showed varying degrees of cross-linked aggregation. As the GA dose increased, the protein gel network became progressively denser and more homogeneous. The other polyphenols showed a more homogeneous network structure at 6 μmol/g_{pro}; however, with a higher dose of polyphenols (ECG/EGCG at 150 μmol/g_{pro}), the protein gels became aggregated and even failed to form a three-dimensional network structure. The above results show that moderate amounts of polyphenols did not disrupt the protein gel network, but high amounts of ECG/EGCG disrupted gel formation. In addition, GA had a significant positive effect on gel network formation. These results reflect cooking loss, gel strength, and WHC (Table 1).

3.10. Molecular docking

Molecular docking was used to further explore how MY interacts with polyphenols to confirm interaction sites. Fig. S4 shows the homology modeling model (Fig. S4.A) and online assessment (Fig. S4.B). Fig. S4 shows that among 808 amino acid residues, 92.6 % were in the most favored region, 6.8 % were in the additional allowed region, 0.4 % were in the allowed region, and only 0.1 % fell in the non-allowed region. Therefore, the model could be considered reliable and was further used for molecular docking studies.

Blind docking was selected due to the unknown protein binding site, and the docking position with the lowest binding energy was chosen as the most representative site. The minimum binding energy of CA, GA, ECG, and EGCG to interact with proteins was −8.8, −6.6, −9.4, and −9.6 kcal/mol, respectively, as shown in Table S2. Therefore, the binding affinity of MY to CA, GA, ECG, and EGCG was arranged in the order EGCG > ECG > CA > GA. The 3D and 2D plots of the interactions of the four polyphenols with the proteins are shown in Fig. 4. As shown in Fig. 4 and Table 2, CA, GA, ECG, and EGCG had 16, 9, 14, and 15 amino acids, respectively, involved in the interaction with proteins; among them, MY formed 5, 4, 5, and 5 hydrogen bonds with CA, GA, ECG, and EGCG. In general, hydrophobic interactions were the dominant force in the interaction of CA, ECG, and EGCG with proteins, and GA had partial hydrophobic interactions with proteins. GA has a relatively simple structure and smoother contact with amino acids in the hydrophobic pocket than the other three polyphenols. At the same time, hydrogen bonds also made the polyphenols more stable with proteins. The results of docking analysis agreed with those of thermodynamic analysis, which was also in line with other scholars' view that protein–polyphenol complex formation is largely dependent on hydrogen bonding and hydrophobic interactions (Dai et al., 2022). However, it was challenging to determine the optimal binding conformation of the proteins to CA, GA, ECG, and EGCG due to the influence of the actual experimental environment (temperature, pH, solvent, etc.). Thus the thermodynamic ΔG value was relatively high (1 kcal ≈ 4.184 kJ) compared to the molecular docking binding energy.

4. Conclusion

In this work, we evaluated the conformational and gel properties of MP influenced by polyphenols (CA, GA, ECG, and EGCG). Multi-spectroscopy and molecular docking techniques were used to explore the interaction mechanisms of the four polyphenols with MP. Polyphenols (CA, GA, ECG, and EGCG) depleted protein sulfhydryl and free amino reactive groups in a dose-dependent manner and caused changes in protein secondary and tertiary structures. Fluorescence spectroscopy analysis showed that polyphenols (CA, GA, ECG, and EGCG) induced MP fluorescence quenching, and the mechanism was static quenching. GA could improve the gel properties of proteins, whereas excess ECG and EGCG led to cross-linked aggregation and prevented the formation of gel networks. Finally, thermodynamic research and molecular docking confirmed that CA, ECG, and EGCG mainly bound to MP via a hydrophobic interaction, but GA and MP were bound primarily via hydrogen bonding. The order of affinity between polyphenols and protein is EGCG > ECG > CA > GA.

CRediT authorship contribution statement

Xin Guo: Formal analysis, Investigation, Methodology, Writing – original draft, Writing – review & editing. **Yabo Wei:** Data curation, Software, Validation. **Pingping Liu:** Formal analysis, Investigation. **Xiaorong Deng:** Supervision, Visualization. **Xinrong Zhu:** Supervision, Visualization. **Zhouping Wang:** Supervision, Validation. **Jian Zhang:** Conceptualization, Funding acquisition, Investigation, Supervision.

Declaration of competing interest

The authors declare that they have no known competing financial interests or personal relationships that could have appeared to influence the work reported in this paper.

Data availability

Data will be made available on request.

Acknowledgments

This research was supported by the National Natural Science Foundation of China (grant numbers 31960460), Key Laboratory for Nutrition and Safety of Xinjiang Specialty Foods, Shihezi City of Eighth Division (grant numbers 2022PT02), Key Laboratory for Agricultural Products Processing Engineering of Shihezi University (grant numbers KYPT201904), and Shihezi University High-level Talent Research Initiation Project (grant numbers RCZK201921) for funding.

Appendix A. Supplementary data

Supplementary data to this article can be found online at https://doi.org/10.1016/j.fochx.2023.101063.

References

Abdur, R. M. (2021). Delineating the interaction mechanism of glabridin and ovalbumin by spectroscopic and molecular docking techniques. *Food Chemistry, 347*, Article 128981. https://doi.org/10.1016/j.foodchem.2020.128981

Bhimaneni, S. P., Bhati, V., Bhosale, S., & Kumar, A. (2021). Investigates interaction between abscisic acid and bovine serum albumin using various spectroscopic and in-silico techniques. *Journal of Molecular Structure, 1224*, Article 129018. https://doi.org/10.1016/j.molstruc.2020.129018

Cao, Y., Ai, N., True, A. D., & Xiong, Y. L. (2018). Effects of (-)-epigallocatechin-3-gallate incorporation on the physicochemical and oxidative stability of myofibrillar protein-soybean oil emulsions. *Food Chemistry, 245*(15), 439–445. https://doi.org/10.1016/j.foodchem.2017.10.111

Cao, Y., & Xiong, Y. L. (2015). Chlorogenic acid-mediated gel formation of oxidatively stressed myofibrillar protein. *Food Chemistry, 180*, 235–243. https://doi.org/10.1016/j.foodchem.2015.02.036

Cao, Y., Xiong, Y. L., Cao, Y., & True, A. D. (2018). Interfacial properties of whey protein foams as influenced by preheating and phenolic binding at neutral pH. *Food Hydrocolloids, 82*, 379–387. https://doi.org/10.1016/j.foodhyd.2018.04.020

Cao, Y., & Xiong, Y. L. (2017). Interaction of whey proteins with phenolic derivatives under neutral and Acidic pH conditions. *Journal of Food Science, 82*(1–3), 409–419. https://doi.org/10.1111/1750-3841.13607

Dai, T., McClements, D. J., Hu, T., Chen, J., He, X., Liu, C., … Sun, J. (2022). Improving foam performance using colloidal protein–polyphenol complexes: Lactoferrin and tannic acid. *Food Chemistry, 377*, Article 131950. https://doi.org/10.1016/j.foodchem.2021.131950

Frazier, R. A., Deaville, E. R., Green, R. J., Stringano, E., Willoughby, I., Plant, J., & Mueller-Harvey, I. (2010). Interactions of tea tannins and condensed tannins with proteins. *Journal of Pharmaceutical and Biomedical Analysis, 51*(2), 490–495. https://doi.org/10.1016/j.jpba.2009.05.035

Han, J., Du, Y., Yan, J., Jiang, X., Wu, H., & Zhu, B. (2021). Effect of non-covalent binding of phenolic derivatives with scallop (Patinopecten yessoensis) gonad protein isolates on protein structure and in vitro digestion characteristics. *Food Chemistry, 357*, Article 129690. https://doi.org/10.1016/j.foodchem.2021.129690

Hao, L., Sun, J., Pei, M., Zhang, G., Li, C., Li, C., … Liu, L. (2022). Impact of non-covalent bound polyphenols on conformational, functional properties and in vitro digestibility of pea protein. *Food Chemistry, 383*, Article 132623. https://doi.org/10.1016/j.foodchem.2022.132623

Hasni, I., Bourassa, P., Hamdani, S., Samson, G., Carpentier, R., & Tajmir-Riahi, H.-A. (2011). Interaction of milk α- and β-caseins with tea polyphenols. *Food Chemistry, 126*(2), 630–639. https://doi.org/10.1016/j.foodchem.2010.11.087

He, B., Ming, Y., Pu, Y., Sun, Y., Jin, M., Yu, C., & Qi, H. (2020). The dual effects of riboflavin and kelp polyphenol extracts on the gel properties of myofibrillar protein from Scomberomorus Niphonius under UVA irradiation. *Food Chemistry, 332*, Article 127373. https://doi.org/10.1016/j.foodchem.2020.127373

Hu, Y., Gao, Y., Solangi, I., Liu, S., & Zhu, J. (2022). Effects of tea polyphenols on the conformational, functional, and morphological characteristics of beef myofibrillar proteins. *LWT, 154*, Article 112596. https://doi.org/10.1016/j.lwt.2021.112596

He, Z., Xu, M., Zeng, M., Qin, F., & Chen, J. (2016). Interactions of milk α- And β-casein with malvidin-3-O-glucoside and their effects on the stability of grape skin anthocyanin extracts. *Food Chemistry., 199*, 314–322. https://doi.org/10.1016/j.foodchem.2015.12.035

Jiang, J., Zhang, Z., Zhao, J., & Liu, Y. (2018). The effect of non-covalent interaction of chlorogenic acid with whey protein and casein on physicochemical and radical-scavenging activity of in vitro protein digests. *Food Chemistry, 268*, 334–341. https://doi.org/10.1016/j.foodchem.2018.06.015

Joye, I. J., Davidov-Pardo, G., Ludescher, R. D., & McClements, D. J. (2015). Fluorescence quenching study of resveratrol binding to zein and gliadin: Towards a more rational approach to resveratrol encapsulation using water-insoluble proteins. *Food Chemistry, 185*, 261–267. https://doi.org/10.1016/j.foodchem.2015.03.128

Khan, S., Zafar, A., & Naseem, I. (2019). Probing the interaction of a coumarin-di(2-picolyl)amine hybrid drug-like molecular entity with human serum albumin: Multiple spectroscopic and molecular modeling techniques. *Spectrochimica Acta Part A: Molecular and Biomolecular Spectroscopy, 223*, Article 117330. https://doi.org/10.1016/j.saa.2019.117330

Li, Y., Liu, H., Liu, Q., Kong, B., & Diao, X. (2019). Effects of zein hydrolysates coupled with sage (salvia officinalis) extract on the emulsifying and oxidative stability of myofibrillar protein prepared oil-in-water emulsions. *Food Hydrocolloids, 87*, 149–157. https://doi.org/10.1016/j.foodhyd.2018.07.052

Liu, P., Zhang, Z., Guo, X., Zhu, X., Mao, X., Guo, X., Deng, X., & Zhang, J. (2021). μ-Calpain oxidation and proteolytic changes on myofibrillar proteins from Coregonus Peled in vitro. *Food Chemistry, 361*, Article 130100. https://doi.org/10.1016/j.foodchem.2021.130100

Moeiniafshari, A.-A., Zarrabi, A., & Bordbar, A.-K. (2015). Exploring the interaction of naringenin with bovine beta-casein nanoparticles using spectroscopy. *Food Hydrocolloids, 51*, 1–6. https://doi.org/10.1016/j.foodhyd.2015.04.036

Pan, J., Lian, H., Jia, H., Li, S., Hao, R., Wang, Y., Zhang, X., & Dong, X. (2020). Ultrasound treatment modified the functional mode of gallic acid on properties of fish myofibrillar protein. *Food Chemistry, 320,* 126637. https://doi.org/ 10.1016/j.foodchem.2020.126637.

Patil, S., Sandberg, A., Heckert, E., Self, W., & Seal, S. (2007). Protein adsorption and cellular uptake of cerium oxide nanoparticles as a function of zeta potential. *Biomaterials, 28*(31), 4600–4607. https://doi.org/10.1016/j.biomaterials.2007.07.029

Pessato, T. B., Carvalho, N. C. D, Tavano, O. L., Fernandes, L. G. R., Zollner, R. D. L., & Netto, F. M. (2016). Whey protein isolate hydrolysates obtained with free and immobilized Alcalase: Characterization and detection of residual allergens. *Food Research International, 83*, 112–120. https://doi.org/10.1016/j.foodres.2016.02.015

Ross, P. D., & Subramanian, S. J. B. J. (1980). Thermodynamics of macromolecular association reactions: Analysis of forces contributing to stabilization. *Biophysical Journal, 32*(1), 79–81. https://doi.org/10.1016/S0006-3495(80)84918-6

Shang, A., Li, J., Zhou, D.-D., Gan, R.-Y., & Li, H.-B. (2021). Molecular mechanisms underlying health benefits of tea compounds. *Free Radical Biology and Medicine, 172*, 181–200. https://doi.org/10.1016/j.freeradbiomed.2021.06.006

Sui, X., Sun, H., Qi, B., Zhang, M., Li, Y., & Jiang, L. (2018). Functional and conformational changes to soy proteins accompanying anthocyanins: Focus on covalent and non-covalent interactions. *Food Chemistry, 245*, 871–878. https://doi.org/10.1016/j.foodchem.2017.11.090

Taotao, D., Jun, C., David, J., & McClements, P. (2019). Protein-polyphenol interactions enhance the antioxidant capacity of phenolics: Analysis of rice glutelin-p-rocyanidin dimer interactions. *Food & Function, 10*(2), 765. https://doi.org/10.1039/c8fo02246a

Wang, H., Xia, X., Yin, X., Liu, H., Chen, Q., & Kong, B. (2021). Investigation of molecular mechanisms of interaction between myofibrillar proteins and 1-heptanol by multiple spectroscopy and molecular docking methods. *International Journal of Biological Macromolecules, 193*, 672–680. https://doi.org/10.1016/j.ijbiomac.2021.10.105

Wang, M., Chen, L., Han, B., Wang, R., Liu, Y., Fan, X., … Mazurenko, I. (2022). Effects of NaCl on the interactions between neomethyl hesperidin dihydrochalcone and pork myofibrillar protein: Their relevance to gelation properties. *Food Research International, 162*, Article 111983. https://doi.org/10.1016/j.foodres.2022.111983

Wang, Y., Liu, M., Zhou, X., Zang, H., Zhang, R., Yang, H., … Shan, A. (2022). Oxidative stability and gelation properties of myofibrillar protein from chicken breast after post-mortem frozen storage as influenced by phenolic compound-pterostilbene. *International Journal of Biological Macromolecules, 221*, 1271–1281. https://doi.org/10.1016/j.ijbiomac.2022.09.088

Wei, Y., Chen, P., Ling, T., Wang, Y., Dong, R., Zhang, C., … Wan, X. J. F. C. (2016). Certain (-)-epigallocatechin-3-gallate (EGCG) auto-oxidation products (EAOPs) retain the cytotoxic activities of EGCG. *Food Chemistry, 204*(1), 218–226. https://doi.org/10.1016/j.foodchem.2016.02.134

Xu, J., Hao, M., Sun, Q., & Tang, L. (2019). Comparative studies of interaction of β-lactoglobulin with three polyphenols. *International Journal of Biological Macromolecules, 136*, 804–812. https://doi.org/10.1016/j.ijbiomac.2019.06.053

Yan, S., Wang, Q., Yu, J., Li, Y., & Qi, B. (2023). Soy protein interactions with polyphenols: Structural and functional changes in natural and cationized forms. *Food Chemistry: X, 19,* 100866. https://doi.org/ 10.1016/j.fochx.2023.100866.

Yang, J., Zhao, Y., Shan, B., Duan, Y., Zhou, J., Cai, M., & Zhang, H. (2023). Study on the interaction and functional properties of Dolichos lablab L. protein-tea polyphenols complexes. *International Journal of Biological Macromolecules, 250*, Article 126006. https://doi.org/10.1016/j.ijbiomac.2023.126006

Zahirović, A., Žilić, D., Pavelić, S., Hukić, M., Muratović, S., & Harej, A. (2019). Type of complex–BSA binding forces affected by different coordination modes of alliin in novel water-soluble ruthenium complexes. *New Journal of Chemistry, 43*(15), 5791–5804. https://doi.org/10.1039/c9nj00826h

Zeng, L., Zhang, G., Lin, S., & Gong, D. (2016). Inhibitory mechanism of apigenin on α-glucosidase and synergy analysis of flavonoids. *Journal of Agricultural & Food Chemistry*. https://doi.org/10.1021/acs.jafc.6b02314

Zhang, Y., Lu, Y., Yang, Y., Li, S., Wang, C., Wang, C., & Zhang, T. (2021). Comparison of non-covalent binding interactions between three whey proteins and chlorogenic acid: Spectroscopic analysis and molecular docking. *Food Bioscience, 41*, Article 101035. https://doi.org/10.1016/j.fbio.2021.101035

Zhang, Z., Liu, P., Deng, X., Guo, X., Mao, X., Guo, X., & Zhang, J. (2021). Effects of hydroxyl radical oxidation on myofibrillar protein and its susceptibility to μ-calpain proteolysis. *LWT, 137*, Article 110453. https://doi.org/10.1016/j.lwt.2020.110453

Zhou, Z., Wang, D., Xu, X., Dai, J., Lao, G., Zhang, S., … Sun, Q. (2023). Myofibrillar protein-chlorogenic acid complexes ameliorate glucose metabolism via modulating gut microbiota in a type 2 diabetic rat model. *Food Chemistry, 409*, Article 135195. https://doi.org/10.1016/j.foodchem.2022.135195